

Mutational and Structural Analyses of the Ribonucleotide Reductase Inhibitor Sml1 Define Its Rnr1 Interaction Domain Whose Inactivation Allows Suppression of *mec1* and *rad53* Lethality

XIAOLAN ZHAO,¹ BILYANA GEORGIEVA,¹ ANDREI CHABES,² VLADIMIR DOMKIN,² JOHANNES H. IPPEL,³ JÜRGEN SCHLEUCHER,³ SYBREN WIJMENGA,³ LARS THELANDER,² AND RODNEY ROTHSTEIN^{1*}

¹Department of Genetics & Development, Columbia University, College of Physicians & Surgeons, New York, New York 10032, ²and Department of Medical Biosciences² and Department of Medical Biochemistry and Medical Biophysics,³ Umeå University, Umeå, SE-90187, Sweden

Received 21 July 2000/Returned for modification 30 August 2000/Accepted 15 September 2000

In budding yeast, *MEC1* and *RAD53* are essential for cell growth. Previously we reported that *mec1* or *rad53* lethality is suppressed by removal of Sml1, a protein that binds to the large subunit of ribonucleotide reductase (Rnr1) and inhibits RNR activity. To understand further the relationship between this suppression and the Sml1-Rnr1 interaction, we randomly mutagenized the *SML1* open reading frame. Seven mutations were identified that did not affect protein expression levels but relieved *mec1* and *rad53* inviability. Interestingly, all seven mutations abolish the Sml1 interaction with Rnr1, suggesting that this interaction causes the lethality observed in *mec1* and *rad53* strains. The mutant residues all cluster within the 33 C-terminal amino acids of the 104-amino-acid-long Sml1 protein. Four of these residues reside within an alpha-helical structure that was revealed by nuclear magnetic resonance studies. Moreover, deletions encompassing the N-terminal half of Sml1 do not interfere with its RNR inhibitory activity. Finally, the seven *sml1* mutations also disrupt the interaction with yeast Rnr3 and human R1, suggesting a conserved binding mechanism between Sml1 and the large subunit of RNR from different species.

Ribonucleotide reductase (RNR) is a highly conserved enzyme that catalyzes the conversion of nucleoside diphosphates (NDPs) to dNDPs, the rate-limiting step of deoxynucleoside triphosphate (dNTP) formation, and DNA synthesis. Its activity directly affects the balance and the levels of the dNTP pools and subsequently genetic stability (29). Due to its vital importance, RNR is tightly regulated by both cell cycle and environmental cues. At S phase and after DNA damage, RNR activity is up-regulated to provide sufficient and balanced dNTP pools for DNA replication and repair. Mutations interfering with this regulated increase in RNR activity in yeast and humans can lead to growth defects and sensitivity to DNA-damaging agents (12, 32). RNR activity is also subjected to negative regulation, which is equally important. This is underscored by the observation that overexpression of a small subunit of yeast or human RNR in yeast cells causes chromosome instability (27). Presumably, the deleterious effects of rampant RNR activity may be due to decreased DNA polymerase fidelity caused by excess dNTP levels and, at the same time, diminished NTP levels, which may interfere with RNA synthesis and numerous ATP/GTP-dependent cellular processes.

Currently, two mechanisms for RNR regulation are known. First, RNR is under allosteric control. In most organisms, the RNR holoenzyme is a tetramer composed of two distinct subunits ($\alpha_2\beta_2$), both of which contribute to the enzymatic activity. However, only the large subunit contains two allosteric sites: one regulates the balance among the four dNTP pools, and the other regulates feedback inhibition by monitoring the dATP/ATP ratio and modulating overall RNR activity accordingly

(20). Second, RNR is subjected to transcriptional regulation. In the budding yeast, transcription of the *RNR* genes is induced in S phase and after DNA damage (10, 11, 12, 17). The induction in S phase is mediated by the *MBP1/SW16* pathway (8, 21); the induction in response to DNA damage is controlled by the *MEC1/RAD53* cell cycle checkpoint pathway (9, 17). This latter pathway can activate a downstream kinase, Dun1, which in turn relieves transcriptional repression by Crt1 (18, 36). In humans, transcription of the RNR large subunit and one RNR small subunit is also induced at S phase (28). Recently, a new human RNR small subunit (p53R2) was shown to be induced by p53 after DNA damage. Moreover, the p53-dependent induction of p53R2 is crucial for DNA repair and cell survival after DNA damage (32).

It is noteworthy that the conservation of RNR from yeast to humans extends beyond the sequence level to include the mechanism of transcriptional regulation via conserved DNA damage checkpoint pathways. Yeast Mec1 is a homolog of ATM (ataxia telangiectasia mutated) and ATR (ataxia- and Rad-related) in humans (16); yeast Rad53 is the homolog of CHK2 in humans, which is mutated in some Li-Fraumeni syndrome patients (2, 26). Both ATM-ATR and CHK2 function upstream of p53 in the DNA damage response (3). From an evolutionary perspective, the conservation of this pathway and its components underscores the importance of dNTP regulation in cell survival.

Recently, a protein inhibitor of RNR has been discovered in yeast. A study of a suppressor of *mec1* and *rad53* lethality (*sml1*) showed that the *SML1* gene negatively regulates dNTP levels (35). Furthermore, it was demonstrated that the Sml1 protein binds to a large subunit of RNR (Rnr1) in vivo and in vitro and inhibits RNR activity efficiently (5, 35). These results suggest a new mode of RNR regulation: Mec1 and Rad53 are required to relieve the Sml1-Rnr1 interaction in S phase, allowing synthesis of sufficient amounts of dNTPs for DNA rep-

* Corresponding author. Mailing address: Department of Genetics & Development, Columbia University, College of Physicians & Surgeons, 701 West 168th St., New York, NY 10032. Phone: (212) 305-1733. Fax: (212) 923-2090. E-mail: rothstein@cuccfa.ccc.columbia.edu.

TABLE 1. Primers used in this study

Primer	Sequence
sml1-mut5'	TACCCATACGATGTTCCAGATTACGCTAGCTTGGGTGGTCATATGGCTGCTCAGTGCGAATTCACC
sml1-mut3'	GTTTTTCAGTATCTACGATTCATAGATCTCTCGAGCTCGAATTCAAGAGTATGAAAGGAACCTTAG
pACTII-GAD5'	TTGGAATCACTACAGGGATG
pACTII-tm	AACCTCTGGCGAAGAAGTCC
SML1start	ATGGAGGCCCGGGGATCCGGATGCAAAATTCGAAGACTAC
SML1stop	CTAGTGGGAAATGGAAGAGAAAAGAAAGAGTATGAAAGGAACCTTTAG
K.L. start	TTCTTTTCTCTTTCCATTTCCACTAGGTGATTCTGGGTAGAAGATCG
K.L. stop	CCGGATCCCGGGGCTCCATTTTCGATGATGTAGTTTCTGG
K.L. 5'int ^a	CTTGACGTTTCGTTTCGACTGATGAGCA
K.L. 3'int ^a	GAGCAATGAACCCAATAACGAAATC
HuR1 5'+1	ACCATCGATGATGCATGTGATCAAGCGAG
HuR1 3'+0	AACGTCAGTCAGGATCCACACATCAGAC
RNR3-5'+0	GAAGGCCTATGTACGTTATTAAGAGACG
RNR3-3'	CGGAAGATCTTTTCTTCTACACCCAGAG
DUN1ORF5'	GGGGATCCAGATGAGTTTGTCCACGAAAAG
DUN13'	AGAGCTGCAGGAGAAAAGTAG
R72A dir	GGGAAAAAGATTGGAGGAGGCACTCAACTCTATCGATC
R72A rev	GATCGATAGAGTTGAGTGCCTCCTCCAAATCCTTTTCCC
L73A dir	GGGAAAAGGATTGGAGGAGAGAGCCAACTCTATCGATCATGACATG
L73A rev	CATGTCATGATCGATAGAGTTGGCTCTCTCCTCCAAATCCTTTTCCC
S75A dir	GGGAAAAGGATTGGAGGAGAGACTCAACGCTATCGATCATGACATG
S75A rev	CATGTCATGATCGATAGCGTTGAGTCTCTCCTCCAAATCCTTTTCCC
S75P dir	GGGAAAAGGATTGGAGGAGAGACTCAACCTATCGATCATGACATG
S75P rev	CATGTCATGATCGATAGGGTTGAGTCTCTCCTCCAAATCCTTTTCCC
F104L dir	GGTCGAGGAAATGGACTTGTAAAGATCCGGCTGC
F104L rev	GCAGCCGGATCCTTACAAGTCCATTTCCTCGACC
Δ2-39dir	TATGGCTGAGGTACCTATGTTGTCTACTCAAAACTC
Δ2-39rev	CATGGAGTTTGTAGTAGACAACATAGGTACCTCAGCCA

^a K.L. 5'int and K.L. 3'int are used in reference 13.

lication. According to this model, in the absence of Mec1 or Rad53, decreased activity of RNR due to constitutive inhibition by Sml1 may cause insufficient dNTP levels and subsequent cell death (35).

The aforementioned model suggests a new mode of RNR regulation and provides a simple explanation for the essential function of Mec1 and Rad53. However, based on current data, other possibilities cannot be excluded. In particular, is suppression of *mec1* and *rad53* lethality by *sml1* mutations really due to loss of RNR inhibition or is there yet another unidentified mechanism(s)? The existing *sml1* alleles do not help differentiate between these possibilities since both are null mutations: one is a deletion of the *SML1* open reading frame (ORF) (*sml1Δ*) and the other is a deletion of its promoter (*sml1-1*) (35). Either mutation may abolish other unknown functions of Sml1 to relieve *mec1* and *rad53* lethality. Additionally, other genetic suppressors of *mec1* and *rad53* lethality, namely overexpression of *RNR1* or deletion of the transcriptional repressor *CRT1* (7, 18), are also not informative, as they likely increase the amount of Rnr1 which titrates Sml1 activity.

Here, we address the above issue by reasoning that if inhibition of RNR by Sml1 leads to inviability in *mec1* and *rad53* cells, then loss-of-function missense mutations of Sml1 should either fail to interact with Rnr1 or abolish its RNR inhibitory activity. Therefore, we performed a comprehensive screening that permits the identification of any *sml1* missense mutation that rescues *mec1Δ* and *rad53Δ* lethality but does not affect protein levels. Next, we asked whether such mutated forms of Sml1 could bind to Rnr1 and inhibit RNR activity. Using such an approach, we obtained seven *sml1* missense mutations. Interestingly, all of these mutations mapped to the last 33 amino acid residues and they all abolish the Sml1-Rnr1 interaction in a two-hybrid assay. Moreover, four mutations were tested in an in vitro RNR assay, and all four no longer inhibit the enzyme.

These results demonstrate that the loss of Sml1-Rnr1 interaction is sufficient to suppress *mec1* and *rad53* lethality.

In addition, the C-terminal clustering of seven Sml1 mutations suggests that this region may contain important structures. Investigation by nuclear magnetic resonance (NMR) studies revealed that the 104-amino-acid-residue-long Sml1 polypeptide has a loosely folded tertiary structure with an N- and a C-terminal alpha helix oriented in an antiparallel fashion. All seven *sml1* missense mutations reside in or are adjacent to the C-terminal alpha helix. Deletion analysis further confirmed that only the C-terminal half of Sml1 is required for inhibition of RNR activity. Taken together, these in vivo and in vitro data define the Rnr1 interaction domain of Sml1. Interestingly, all seven *sml1* mutations also abolished the interaction with the other yeast RNR large subunit (Rnr3) as well as with the human RNR large subunit, suggesting a conserved binding mechanism for these interactions.

MATERIALS AND METHODS

Primers, yeast strains, and plasmids. All primers used in this study are listed in Table 1. We used the cloning-free PCR-based allele replacement method to integrate two mutant alleles at the *SML1* chromosomal locus (13). In brief, mutant *sml1* ORFs (*sml1-176T* and *sml1-S87P*) were amplified using primer pair SML1start and SML1stop. Fragments containing the N-terminal or C-terminal two-thirds of the *Kluyveromyces fragilis* *URA3* gene were amplified using primer pairs K.L. start and K.L. 3'int or K.L. stop and K.L. 5'int, respectively. Each of these two PCR products was fused to the *sml1* ORF by mixing the appropriate fragments and amplifying using primer pairs SML1start and K.L. 3'int or SML1stop and K.L. 5'int. The final fusion products were gel purified and co-transformed into a wild-type yeast strain W1588-4A (35; all yeast strains used in this study, except PJ69-4A, are in the W303 background and only the relevant genotype is noted). Transformants were selected on synthetic complete (SC)-Ura and recombinants that excised the *K. fragilis* *URA3* gene were obtained on SC-5-fluoroorotic acid medium. The correct replacements were confirmed by PCR and sequence analysis. Two yeast strains constructed by this allele replacement method were crossed to U963-61A (*MATa mec1Δ::TRP1 sml1Δ::HIS3*) and W2105-17B (*MATa rad53Δ::HIS3 sml1Δ::URA3*) to obtain the four diploid

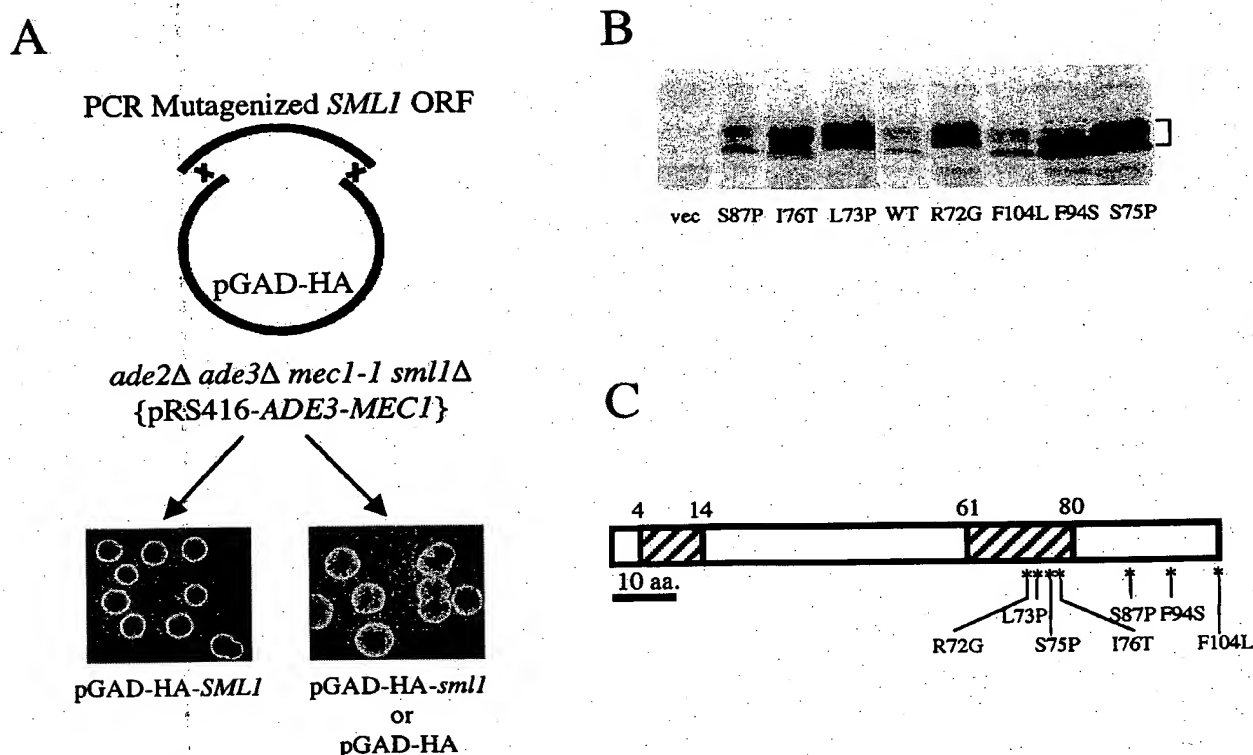


FIG. 1. Isolation of loss-of-function *sm1* mutations. (A) Scheme for isolating loss-of-function *sm1* mutations. The *SML1* ORF was mutagenized by PCR amplification (see Materials and Methods). The PCR fragments were cotransformed into yeast strain U1047 (*MATa ade2Δ ade3Δ sm1Δ::HIS3 mec1-1* [pC87 *ADE3-URA3-MEC1*]) with gapped vector pACT11 that has a GAD fused with an HA tag (pGAD-HA). Strain U1047 forms solid red colonies when the fusion protein contains wild-type *SML1* (pGAD-HA-*SML1*); it forms red-white sectorial colonies when the fusion protein contains loss-of-function *sm1* mutations (pGAD-HA-*sm1*) or only the GAD-HA fusion. (B) Expression of the mutated *Sml1* proteins. The GAD-HA fusion proteins containing wild-type and mutated *Sml1* were detected on a protein blot by using anti-HA antibody (12CA5). The bracket indicates the GAD-HA-*Sml1* proteins. The multiple bands are due to phosphorylation that is stabilized in GAD-HA-*Sml1* fusion proteins (data not shown). (C) Positions of the seven *sm1* mutations. The amino acid (a.a.) changes and their positions on the protein are illustrated. The hatched boxes depict alpha-helical regions revealed by NMR.

strains used in the study (see Fig. 2). During tetrad analysis, *sm1-I76T* and *sm1-S87P* were detected by the absence of a *Clal* site and the presence of a new *AvaII* site, respectively.

Strain PJ69-4A (*MATa trp1-901 leu2-3,112 ura3-52 his3-200 gal4Δ gal80Δ LYS2::GAL1-HIS3 GAL2-ADE2 met2::GAL7-lacZ*) was used as the two-hybrid host strain; vectors pGBD-C1, pGBD-C2, and pGBD-C3 were used to construct the two-hybrid plasmids (19). Human R1 cDNA was PCR amplified from a human liver cDNA library (a gift from Guangxia Gang and Stephen Goff) by using primer pair HuR1 5' +1 and HuR1 3' +0. The PCR fragment was cloned into the pGBD-C3 vector between the *Clal* and *PstI* sites to create pWJ900. The yeast *RNR3* gene was PCR amplified from plasmid pSE734 (kindly provided by Steve Elledge) by using primer RNR3-5' +0 and primer RNR3-3'. The PCR fragment was cloned into the pGBD-C1 vector between the *SmaI* and *BamHI* sites to create pWJ770. The yeast *DUN1* gene was PCR amplified from wild-type chromosomal DNA by using primer DUN1ORF5' and primer DUN13'. The PCR fragment was cloned into the pGBD-C2 vector between the *PstI* and *BamHI* sites to create pWJ730.

To construct *Escherichia coli* expression plasmids that contain *sm1-R72A*, *sm1-L73A*, *sm1-S75A*, *sm1-S75P*, or *sm1-F104L*, the pET3a*SML1* expression plasmid (5) was mutagenized using the QuickChange Site-Directed Mutagenesis Kit (Stratagene). The primer pairs were named according to their corresponding mutations and are listed in Table 1. The correct mutations were confirmed by DNA sequence analysis. To construct the pET3aΔ2-39 *sm1* plasmid, pET3a*SML1* was first cut by the restriction endonucleases *NdeI* and *NcoI*. The 4.77-kb fragment between *NdeI* and *NcoI* was subsequently ligated with the annealed Δ2-39dir and Δ2-39rev oligonucleotides. pET3aΔ28-50 *sm1* was made by self-ligation of the 4.85-kb fragment that was produced from the *NcoI* digestion of the pET3a*SML1* plasmid.

Isolation of loss-of-function *sm1* mutations. PCR mutagenesis of the *SML1* ORF was carried out using the chimeric primers *sm1-mut5'* and *sm1-mut3'*. The 5' 46 nucleotides of these two primers are homologous to sequences adjacent to the *BamHI* and *NcoI* sites on the pACT11 vector (a 2-μm plasmid containing a Gal4 activation domain [GAD] followed by a hemagglutinin [HA]

tag; Clontech Inc.). The 3' sequences of the two primers are homologous to the flanking sequence of the *SML1* ORF. The PCR mixture contained the following components: 10 mM Tris-HCl, 1.5 mM MgCl₂, 50 mM KCl (pH 8.3), 0.25 mM MnCl₂, 500 μM (each) dNTPs, 1 μM concentrations of each primer, 5 U of *Taq* DNA polymerase, and 10 ng of plasmid pWJ699 (35) as template. The PCR conditions were 40 cycles of 30 s at 94°C, 15 s at 54°C, and 1 min at 72°C.

The PCR-mutagenized product was gel purified and cotransformed into yeast strain U1047 (*MATa ade2Δ ade3Δ sm1Δ::HIS3 mec1-1* [pC87 *ADE3-URA3-MEC1*]) with pACT11 vector that was linearized at *BamHI* and *NcoI* sites. In vivo homologous recombination between the PCR fragments and the vector DNA produced a library of fusion proteins composed of GAD and mutagenized *Sml1* (25). The yeast strain U1047 forms red-white sectorial colonies on nonselective medium, as the plasmid pC87 is not required for cell viability and is lost during cell division (22, 30). However, when transformed with plasmid pWJ845 (35), which encodes the GAD-HA-*Sml1* fusion protein, cells cannot lose pC87 plasmid and therefore form solid red colonies (Fig. 1A). When transformed with vector pACT11 alone or with a pGAD-HA-*sm1* mutant plasmid, cells can lose pC87 plasmid and form red-white sectorial colonies (Fig. 1A).

After growing transformants at 30°C for 5 days, red-white sectorial colonies were picked. These candidates were further tested for insertions by colony PCR using primer pair pACT11-GAD5' and pACT11-tm. The self-ligated pACT11 vector gave rise to a 450-bp fragment, while plasmids containing insertions gave rise to a 760-bp fragment. Only plasmids containing insertions were further analyzed for protein levels by protein blottings using anti-HA antibody (12CA5; Boehringer Mannheim). Twelve plasmids producing fusion proteins close to the size of GAD-HA-*Sml1* and at or above wild-type protein levels were rescued from yeast cells and retransformed into strain U1047. Their phenotype and protein levels were confirmed.

Sequence analysis revealed that four of the plasmids contain a single nucleotide change, each resulting in one of the following substitutions: L73P, I76T, S87P, and F104L. Moreover, three plasmids contain mutation R72G, three plasmids contain mutation S75P, and two plasmids contain mutation F94S. Two of the plasmids that have the S75P mutation also contain additional mutations.

Since mutation S75P alone results in the loss of Sml1 function, these plasmids were not further analyzed.

Expression of recombinant Sml1 and generation of anti-Sml1 antibody. Recombinant wild-type and mutant Sml1 proteins were expressed in *E. coli* BL21 (DE3) pLysS bacteria as described by Chabes et al. (5), except for $\Delta 2-39$ Sml1, for which the ammonium sulfate precipitation step was omitted. Isotope labeling of Sml1 was made by growing bacteria in minimal medium containing $^{15}\text{NH}_4\text{Cl}$ and ^{13}C glucose.

The *SML1* ORF was PCR amplified and cloned into vector pQE60 (Qiagen). His₆-tagged Sml1 protein was then purified from *E. coli* extracts by using an Ni-nitrilotriacetic acid column according to the manufacturer's instructions. The purified protein was injected into rabbits to generate polyclonal antibodies (Cocalico Biologicals, Inc.).

NMR spectroscopy. The sequence-specific backbone assignment of the Sml1 protein was derived from standard triple resonance NMR spectra (31) on uniformly labeled ^{15}N -labeled and ^{13}C , ^{15}N -labeled samples. Spectra were recorded at temperatures between 2 and 6°C on Bruker DRX-600 and DMX-500 spectrometers. Samples contained 25 mM sodium phosphate buffer (pH 7.0), 25 mM NaCl, 90% H_2O –10% D_2O , and 10 mM dithiothreitol. Protein concentrations of 0.4 and 0.6 mM were used for the ^{15}N -labeled and ^{13}C , ^{15}N -labeled samples, respectively. Values for random coil shifts used in the calculation of secondary α shifts were taken from a study by Wishart et al. (33). Relaxation studies of ^{15}N were carried out as described by Farrow et al. (14).

Other methods. Yeast media preparation and other yeast manipulations were described by Adams et al. (1). Extraction of yeast proteins and protein blottings were performed as described by Harlow and Lane (15). The RNR activity assay was described by Chabes et al. (4).

RESULTS

Isolation of missense *sml1* mutations that do not inhibit *mec1* cell growth. To understand whether the inhibitory binding of Sml1 to Rnr1 causes lethality in *mec1* null strains, we designed a screen to isolate missense *sml1* mutations that are not toxic in *mec1* cells. In brief, the *SML1* ORF was randomly mutagenized by PCR amplification. The resulting DNA fragments were cotransformed with a gapped two-hybrid vector into a *mec1-1 sml1* strain that also contained a pRS416-*ADE3-MEC1* plasmid (see Materials and Methods). In vivo homologous recombination between the PCR fragments and the vector DNA produced a library of fusion proteins composed of the GAD and mutagenized Sml1. Candidates for loss-of-function *sml1* mutations were identified using the red-white color screen shown in Fig. 1A (also see Materials and Methods). In this scheme, the fusion protein of GAD and wild-type Sml1 gave rise to solid red colonies since a functional Sml1 only allows the growth of cells that retain the *MEC1*-containing plasmid (the *ADE3* marker on this plasmid confers the red color). In contrast, an inactive Sml1 gave rise to red-white sector colonies since the *MEC1*-containing plasmid is inconsequential and can be lost randomly. Sector colonies due to vector self-ligation without incorporation of Sml1 were eliminated by PCR analysis of the insertion (see Materials and Methods). Mutations causing truncations or unstable proteins were also eliminated by examination of the fusion proteins on protein blots. Among 1,200 red-white sector colonies, 12 contained plasmids that produced near-full-length fusion proteins at a level similar to or higher than that of GAD-HA-Sml1 (Fig. 1B). These plasmids were rescued from yeast and confirmed for their effect in *mec1*Δ and *rad53*Δ cells.

Sequence analysis of these 12 plasmids revealed seven substitution mutations: R72G, L73P, S75P, I76T, S87P, F94S, and F104L (Fig. 1C). The R72G, F94S, and S75P missense changes were identified multiple times. Interestingly, all these mutations localized to the 33 C-terminal amino acids of the Sml1 protein (104 amino acids long), suggesting that the C terminus of Sml1 is important in causing *mec1* and *rad53*Δ inviability.

Chromosomal copies of *sml1* mutations also rescue *mec1*Δ and *rad53*Δ lethality. To eliminate any artifacts due to overexpression of Sml1 from the plasmids, two *sml1* mutations (I76T and S87P) were integrated into the chromosomal *SML1*

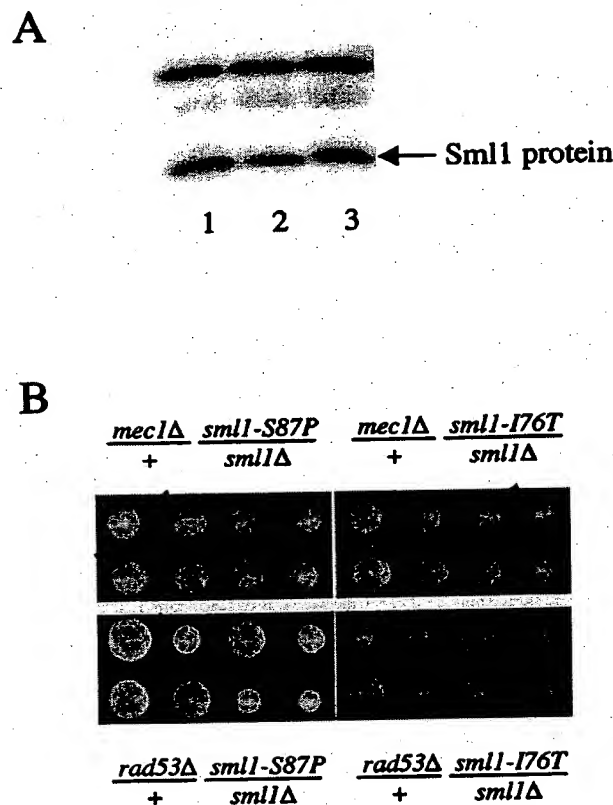


FIG. 2. *sml1* mutations rescue *mec1* and *rad53* lethality. (A) The Sml1 protein level in wild-type (lane 1), *sml1*-I76T (lane 2), and *sml1*-S87P (lane 3) strains was examined by protein blotting. The arrow indicates the Sml1 protein. The darker band above Sml1 cross-reacts to anti-Sml1 serum and was used as a loading control. (B) Tetrad analysis of *sml1*-I76T and *sml1*-S87P. The genotype of the diploid is above or below each panel. Two tetrads are shown for each and are displayed horizontally. The arrows (→) indicate *mec1*Δ *sml1*Δ (top) and *rad53*Δ *sml1*Δ (bottom). The arrowheads (▼) indicate *mec1*Δ *sml1*-S87P (top left), *mec1*Δ *sml1*-I76T (top right), *rad53*Δ *sml1*-S87P (bottom left), and *rad53*Δ *sml1*-I76T (bottom right). In all cases, *sml1*Δ and two *sml1* mutations suppressed *mec1*Δ and *rad53*Δ to a similar degree.

locus to replace the wild-type gene. These mutant alleles produced wild-type levels of protein, indicating that protein stability is unaffected (Fig. 2A). Genetic analysis showed that, like an *sml1*Δ mutation, both *sml1*-I76T and *sml1*-S87P suppress the lethality of *mec1*Δ or *rad53*Δ mutants: they both completely rescue the growth defect of *mec1*Δ cells but only partially rescue that of *rad53*Δ (Fig. 2B). Also similar to *sml1*Δ, these two mutations do not rescue the checkpoint defects of *mec1*Δ or *rad53*Δ strains (data not shown).

***sml1* mutations do not interact with the large subunits of yeast RNR in a two-hybrid assay.** All seven *sml1* mutations were tested in the yeast two-hybrid assay for interaction with the large subunits of the RNR enzyme. In yeast, *RNR1* and *RNR3* encode two large subunits of RNR that have 80% identity (7, 11). We showed previously that wild-type Sml1 interacts with Rnr1 (35). Interestingly, all seven mutated forms of Sml1 failed to interact with Rnr1, as they were unable to turn on any of the three two-hybrid reporter genes (Fig. 3 and data not shown). We have also found that Sml1 interacts with Dun1 in two-hybrid assays, and we used this as a control for nonspecific loss of interaction. The seven mutated proteins, like Sml1-R72G shown in Fig. 3A, still retained their ability to interact

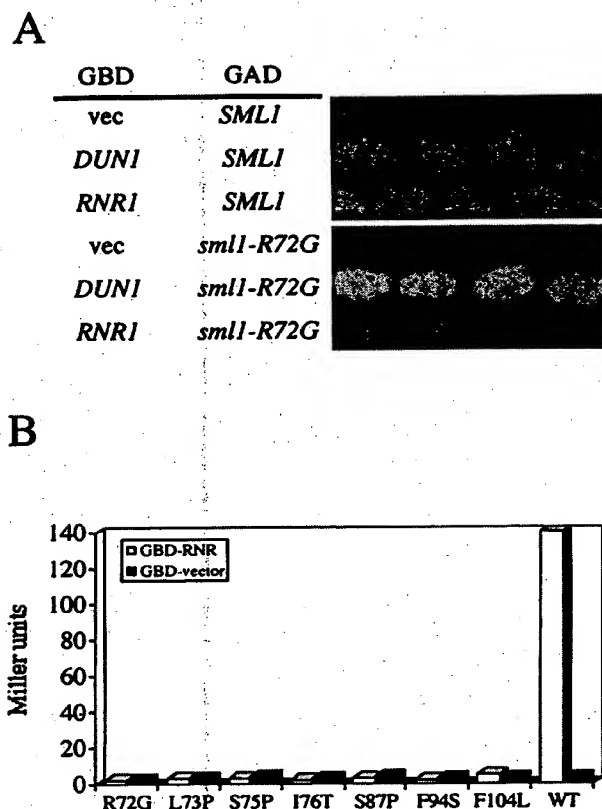


FIG. 3. Interaction between *SML1* or *sm11* mutants and *RNR1* or *DUN1* in two-hybrid assays. (A) Plasmids containing GAD-*HA-SML1* or GAD-*HA-sm11-R72G* were cotransformed with plasmids containing GBD vector alone (vec), GBD-*DUN1*, or GBD-*RNR1* into two-hybrid strain PJ69-4A. The interactions were assayed by activation of the *HIS3* reporter on SC-TRP-LEU-HIS medium. Four or five transformants are shown for each cotransformation. *sm11-R72G* failed to bind to *Rnr1* but still interacted with *Dun1*. Similar observations were made for the other six *sm11* mutations (data not shown). (B) LacZ activity was measured in Miller Units (1). The white bars represent the interactions between *sm11* mutants and *Rnr1*, and the black bars represent those between *sm11* mutants and the empty GBD vector. WT, wild type.

with *Dun1*. Thus, it is likely that these mutations specifically disrupted the *Sml1*-*Rnr1* interaction.

Although *RNR3* is not essential for growth and DNA damage repair, its overexpression can complement *mri1* mutations as well as suppress the lethality of *mec1* and *rad53* (7, 11). These observations indicate that *Rnr3* can functionally substitute for *Rnr1*. In a two-hybrid assay, we observed that the *Rnr1*-*Rnr3* combination only activates the more sensitive *HIS3* reporter gene, suggesting a weak interaction (Fig. 4A). We next tested whether wild-type and mutant forms of *Sml1* can interact with *Rnr3*. As shown in Fig. 4A, wild-type *Sml1* interacted strongly with *Rnr3* while *Sml1*-R72G failed to interact. Similar results were observed with the other six *sm11* mutants (data not shown).

Solution structure of *Sml1* and positions of the mutations in the secondary structure. The locations of the seven mutations suggest that the C terminus of *Sml1* may contain structural elements important for its function. To investigate this further, the three-dimensional structure of the free *Sml1* protein and its dynamics were determined by NMR. Here, we present the structural data most relevant for the interpretation of the mutations. We found that the free *Sml1* polypeptide chain is

highly flexible in solution and has no defined tertiary structure. However, three regions exhibited a high degree of backbone order ($S^2 > 0.6$). These are amino acid residues 4 to 14, 20 to 35, and 61 to 80. Both regions 4 to 14 and 61 to 80 are alpha-helical, as shown by the positive secondary α chemical shifts of the amino acids in these two regions (Fig. 5). Overall, the three-dimensional architecture of *Sml1* is best characterized as a loosely folded tertiary structure in which the two main helices are oriented in an antiparallel fashion. Interestingly, four *Sml1* mutations reside in the 61 to 80 alpha helix and the other three mutations are located in the random coil region C terminal from this helix.

Effects of mutations and deletions in *Sml1* on its inhibitory activity of *RNR*. To understand the biological significance of the structural elements revealed by NMR studies, deletions and mutations of *Sml1* were tested in an in vitro *RNR* activity assay. First, we deleted amino acids 2 to 39, which contain two regions exhibiting high degrees of backbone order (4 to 14 and 20 to 35). This recombinant protein inhibits *RNR* activity in vitro as potently as wild-type *Sml1* (Fig. 6). Next, a deletion was made between amino acid residues 28 and 50, eliminating most of the nonstructural linker region. This truncated protein also efficiently inhibited *RNR* activity (Fig. 6). Thus, the N-terminal half of *Sml1* (amino acids 2 to 50) is not required for *RNR* inhibition. Together with the mutagenesis data, these results clearly demonstrate that the C terminus is necessary and sufficient for the inhibitory role of *Sml1*.

Next, we addressed the question of whether residues R72, L73, and S75 inactivated *Sml1* as a result of the destruction of the alpha helix or the loss of side chain-specific interactions. Each of the original mutations, R72G, L73P, and S75P, was mutated to alanine (R72A, L73A, and S75A) to avoid destabilization of the alpha helix (6). In the in vitro assay, both R72A and L73A lost the ability to inhibit *RNR*, suggesting that

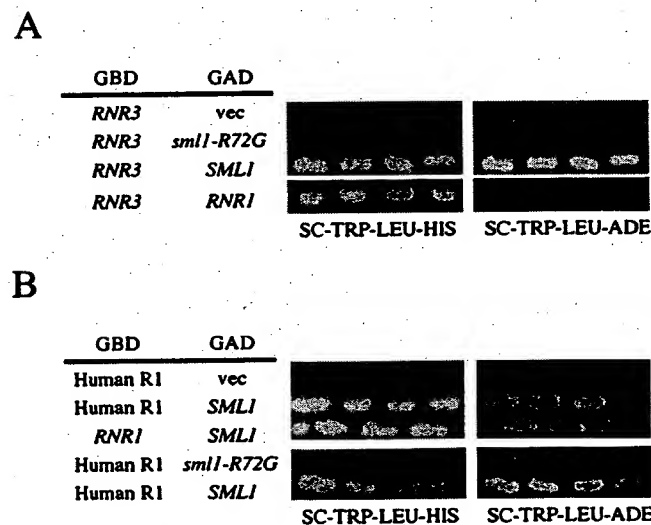


FIG. 4. The *sm11* mutations abolish the interaction with *RNR3* and human R1. Different sets of plasmids were cotransformed into two-hybrid strain PJ69-4A, and the activation of *HIS3* and *ADE2* reporters were examined by growing transformants on SC-TRP-LEU-HIS and SC-TRP-LEU-ADE plates, respectively. (A) The GBD-*RNR3* plasmid was cotransformed into PJ69-4A with plasmids containing either GAD (vec), GAD-*sm11-R72G*, GAD-*SML1*, or GAD-*RNR1*. (B) The GBD-human R1 plasmid was cotransformed into two-hybrid strain PJ69-4A with plasmids containing either GAD (vec), GAD-*SML1*, or GAD-*sm11-R72G*. GBD-*RNR1* and GAD-*SML1* are also included for comparison.

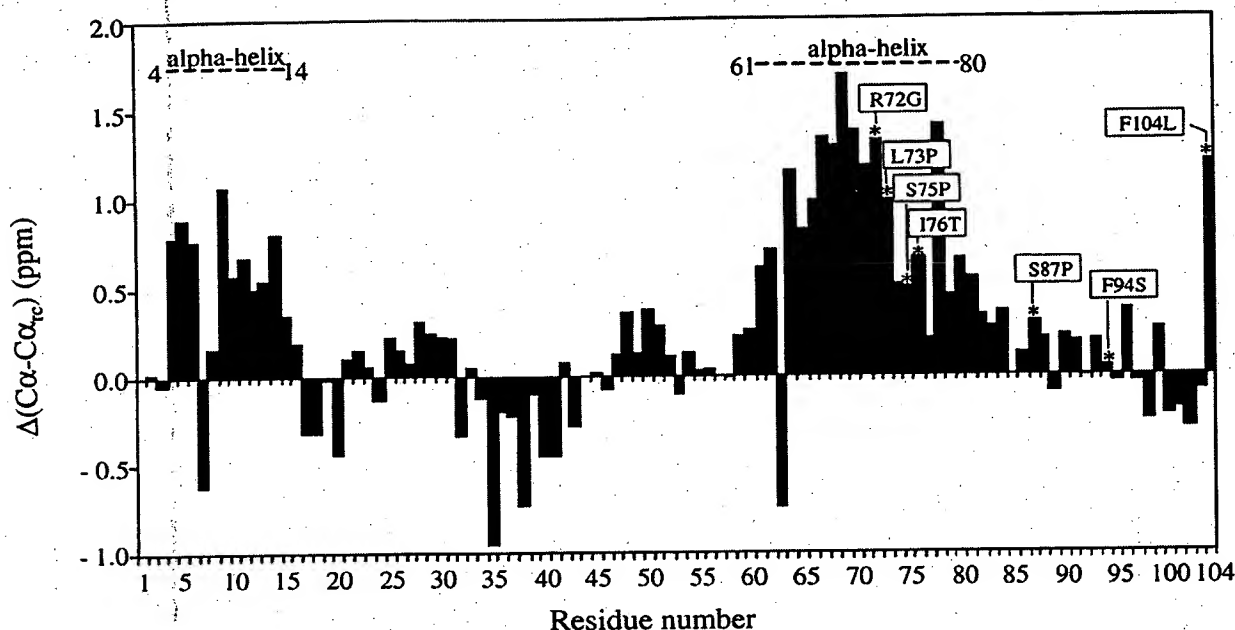


FIG. 5. Secondary $C\alpha$ chemical shifts of individual amino acid residues in Sml1 determined from NMR data. Positive $C\alpha$ values indicate the presence of an alpha helix (shown by dashed lines). The positions of the seven *sml1* mutations are labeled.

R72 and L73 are likely to be involved in side chain-specific interactions (Fig. 6). On the other hand, S75A could still inhibit RNR, while the S75P substitution completely abolished the inhibition (Fig. 6). This result indicates that S75 is important only for maintaining the alpha helix.

We also tested mutation F104L for in vitro inhibition of RNR. This mutation (which resides outside the C-terminal alpha helix) dramatically reduced Sml1 inhibitory activity, suggesting that the random coil downstream of the C-terminal alpha helix also contributes to the regulation of RNR (Fig. 6).

Mutations affecting Sml1 and yeast Rnr1 or Rnr3 interaction abolish Sml1-human R1 interaction. The RNR enzyme has been very conserved throughout evolution (reviewed in reference 20). For example, Rnr1 in yeast has 67% identity and 83% similarity with the large subunit from the mouse and humans. Thus, it is reasonable to expect that yeast Sml1 may interact with RNRs from other species. We showed previously that Sml1 interacts with the large subunit of the mouse RNR in vitro almost as strongly as it does with yeast Rnr1 (5). We now show that Sml1 can also bind to the human large subunit (human R1) in a two-hybrid assay. This interaction is as strong as that of Sml1 and yeast Rnr1, judging by the expression of the three two-hybrid reporters (Fig. 4B; data not shown). We tested the same seven Sml1 mutants required for binding to yeast Rnr1 and Rnr3 for their effect on Sml1-human R1 interaction. All seven failed to interact with the human R1, and an example is shown for Sml1-R72G (Fig. 4B). This suggests that the binding mechanism between Sml1 and the RNR large subunits has been conserved from yeast to humans.

DISCUSSION

The relationship between the Sml1-RNR interaction and Mec1 and Rad53 essential functions. Sml1 was first isolated as a suppressor of *mec1Δ* and *rad53Δ* lethality (35). Study of the *sml1* mutant phenotype suggested that Sml1 negatively regu-

lates dNTP synthesis. Consistent with this idea, deletion of Sml1 results in a 2.5-fold increase of all four dNTPs (35). Two-hybrid and biochemical results further revealed that Sml1 inhibits dNTP synthesis by directly binding to the large subunits of RNR (5, 35). These studies demonstrate clearly that the Sml1 protein functions as an inhibitor of the key enzyme in dNTP formation. However, it was unclear from these experiments whether *sml1* suppression of *mec1* and *rad53* mutants is

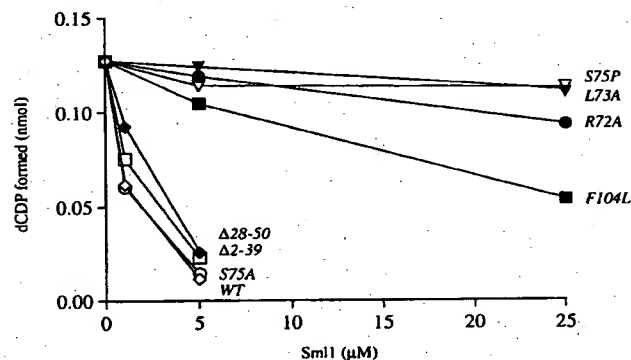


FIG. 6. Effect of Sml1 mutations on its inhibitory activity of RNR. Assay mixtures contained 20 mM HEPES-KOH (pH 7.4), 200 mM potassium acetate, 5 mM ATP, 20 mM magnesium acetate, 1 mM [3 H]CDP (specific activity, 27,000 cpm/nmol), 20 μ M FeCl₃, 20 mM dithiothreitol, 0.2 μ M Rnr1, 1 μ M Rnr2/Rnr4 heterodimer, and the indicated concentrations of recombinant wild-type or mutated Sml1. The reaction mixtures were incubated at 30°C for 20 min in a final volume of 50 μ l. At least two independent assays were performed for each concentration of wild-type and mutant Sml1. After incubation, the samples were processed as described earlier to obtain the amount of dCDP formed (4). Shown are wild-type Sml1 (WT) (open diamond), Δ 28-50 (filled diamond), Δ 2-39 (open square), S75A (open circle), S75P (open triangle), R72A (filled circle), F104L (filled square), and L73A (filled triangle).

due to loss of this function or is due to another unidentified mechanism(s).

To address this issue, we screened for missense *sm11* mutations that relieve the lethality of *mec1* and *rad53* mutant cells and then tested whether these mutations affect Sm11 binding to Rnr1 or inhibition of RNR. We expected that if the inviability in *mec1* or *rad53* cells is due to the inhibition of RNR by Sm11, then *sm11* suppressor mutations should always abolish its RNR inhibitory activity. On the other hand, if the toxicity in *mec1* or *rad53* cells is caused by some other function of Sm11, then these suppressors would not necessarily affect the interaction with Rnr1. Among the *sm11* mutations that suppress *mec1* lethality, we found seven missense mutations that expressed protein at or above wild-type levels. Each of these mutations abolished the interaction with Rnr1 in a two-hybrid assay. Furthermore, they also abolished the interaction with Rnr3, an isoform of the RNR large subunit. However, these mutations did not affect the interaction between Sm11 and Dun1 (which is under further investigation). Therefore, it is likely that the seven Sm11 mutations specifically destroy the interaction of Sm11 with the large RNR subunits. Additionally, four mutations were tested for inhibition of RNR activity in vitro and none showed significant inhibition. Taken together, these results show that mutations of Sm11 residues essential for the interaction between Sm11 and the large subunits of RNR relieve *mec1* and *rad53* inviability.

The structure of Sm11. Sm11 is a small protein of 104 amino acid residues (35). Interestingly, the region necessary and sufficient to inhibit RNR activity is even smaller. The fact that all seven Sm11 mutations that failed to interact with Rnr1 and Rnr3 are located within the last 33 amino acids and that deletion of the first 50 amino acids did not affect inhibition of RNR activity suggests that only the C-terminal half of Sm11 is important for RNR inhibition. NMR studies show that this region contains a long alpha helix (amino acids 61 to 80) where four mutations (R72G, L73P, S75P, and I76T) reside (Fig. 5). The alpha helix-breaking S75P mutation, but not the S75A mutation, inactivates Sm11, indicating the importance of this helix. However, the inability of the three mutations downstream of this helix, S87P, F94S, and F104L, to bind to Rnr1 or Rnr3 reveals the presence of additional interfaces between Sm11 and Rnr1.

NMR studies also revealed two other regions of the Sm11 protein that exhibit a high degree of backbone order (4 to 14 and 20 to 35). However, deletion of these regions does not affect Sm11 inhibitory activity in vitro. It will be of interest to see whether these regions are involved in other aspects of Sm11 regulation (e.g., protein modification). Apart from three local structural elements, overall, the Sm11 protein in solution lacks a defined global structure. The three-dimensional architecture of Sm11 is best characterized as a loosely folded structure in which the two main helices are oriented in an antiparallel fashion. The significance of such a loosely folded structure remains to be determined. However, an increasing number of studies show that many regulatory proteins lack global structure (reviewed in reference 34). For example, the cyclin-dependent kinase inhibitor p21^{Waf1/Cip1/Sdi1} is soluble and stable but shows no evidence of tertiary structure in NMR studies (23). Similar cases were found among transcription and translation factors as well as proteins that are involved in membrane fusion (reviewed in reference 34). An intrinsically unfolded structure is thought to serve a critical role in protein binding and to provide a simple mechanism for regulation through modification. This feature is also thought to permit rapid turnover, allowing a quick response to environmental stimuli (34).

Perhaps the loosely folded Sm11 structure is important for its regulation by Mec1 and Rad53.

Although no homology of Sm11 has yet been reported, our earlier studies showed that Sm11 binds to the mouse R1 protein nearly as strongly as to yeast Rnr1 (5). Here we show that yeast Sm11 binds to the large subunit of human RNR and that the same Sm11 residues essential for the yeast RNR interaction are also required for binding the human protein. Thus, it is likely that Sm11 interacts with yeast and mammalian R1 through a similar mechanism. Further structural studies of the complexes between Sm11 and RNR large subunits from different species will hopefully reveal the mechanism of inhibition. This type of information will be important for designing anticancer drugs targeting RNR since increased RNR activity is often associated with rapidly proliferating tumor cells. Recently, it was shown that a lack of p53R2 induction in p53-deficient cells causes sensitivity to DNA damage (32). This led to the proposal that the low residual resistance seen in p53-deficient cells is due to basal-level dNTP synthesis (24). If this is true, then p53-deficient cancer cells may be selectively sensitized by the combination of DNA-damaging chemotherapeutic agents and a Sm11-like inhibitor that binds to the RNR large subunit to eliminate basal RNR activity.

ACKNOWLEDGMENTS

We are grateful to Marisa Wagner for critically reading the manuscript.

This work was supported by National Institutes of Health grant GM50237 (R.R.), by the Alexander and Margaret Stewart Trust Pilot Project in Cancer Research (X.Z. and R.R.), by the Swedish Natural Sciences Research Council (S.W. and L.T.), and by The Royal Swedish Academy of Sciences (V.D.).

REFERENCES

- Adams, A., D. E. Gottschling, C. A. Kaiser, and T. Stearns. 1997. Methods in yeast genetics, a Cold Spring Harbor Laboratory course manual. Cold Spring Harbor Laboratory Press, Cold Spring Harbor, N.Y.
- Bell, D. W., J. M. Varley, T. E. Szidlo, D. H. Kang, D. C. Wahrer, K. E. Shannon, M. Lubratovich, S. J. Verselis, K. J. Isselbacher, J. F. Fraumeni, J. M. Birch, F. P. Li, J. E. Garber, and D. A. Haber. 1999. Heterozygous germ line hCHK2 mutations in Li-Fraumeni syndrome. *Science* 286:2528-2531.
- Caspari, T. 2000. How to activate p53. *Curr. Biol.* 10:R315-R317.
- Chabes, A., V. Domkin, G. Larsson, A. Liu, A. Graslund, S. Wijmenga, and L. Thelander. 2000. Yeast ribonucleotide reductase has a heterodimeric iron-radical-containing subunit. *Proc. Natl. Acad. Sci. USA* 97:2474-2479.
- Chabes, A., V. Domkin, and L. Thelander. 1999. Yeast Sm11, a protein inhibitor of ribonucleotide reductase. *J. Biol. Chem.* 274:36679-36683.
- Chou, P. Y., and G. D. Fasman. 1978. Empirical predictions of protein conformation. *Annu. Rev. Biochem.* 47:251-276.
- Desany, B. A., A. A. Alcasabas, J. B. Bachant, and S. J. Elledge. 1998. Recovery from DNA replication stress is the essential function of the S-phase checkpoint pathway. *Genes Dev.* 12:2956-2970.
- Dirick, L., T. Moll, H. Auer, and K. Nasmyth. 1992. A central role for Swi6 in modulating cell cycle Start-specific transcription in yeast. *Nature* 357:508-513.
- Elledge, S. J. 1996. Cell cycle checkpoints: preventing an identity crisis. *Science* 274:1664-1672.
- Elledge, S. J., and R. W. Davis. 1989. DNA damage induction of ribonucleotide reductase. *Mol. Cell. Biol.* 9:4932-4940.
- Elledge, S. J., and R. W. Davis. 1990. Two genes differentially regulated in the cell cycle and by DNA-damaging agents encode alternative regulatory subunits of ribonucleotide reductase. *Genes Dev.* 4:740-751.
- Elledge, S. J., Z. Zhou, J. B. Allen, and T. A. Navas. 1993. DNA damage and cell cycle regulation of ribonucleotide reductase. *Bioessays* 15:333-339.
- Erdeniz, N., U. H. Mortensen, and R. Rothstein. 1997. Cloning-free PCR-based allele replacement methods. *Genome Res.* 7:1174-1183.
- Farrow, N. A., O. Zhang, A. Szabo, D. A. Torchia, and L. E. Kay. 1995. Spectral density function mapping using ¹⁵N relaxation data exclusively. *J. Biomol. NMR* 6:153-162.
- Harlow, E., and D. Lane. 1988. Antibodies, a laboratory manual. Cold Spring Harbor Laboratory Press, Cold Spring Harbor, N.Y.
- Hoekstra, M. F. 1997. Responses to DNA damage and regulation of cell cycle checkpoints by the ATM protein kinase family. *Curr. Opin. Genet. Dev.* 7:170-175.

17. Huang, M., and S. J. Elledge. 1997. Identification of *RNR4*, encoding a second essential small subunit of ribonucleotide reductase in *Saccharomyces cerevisiae*. *Mol. Cell. Biol.* 17:6105–6113.
18. Huang, M., Z. Zhou, and S. J. Elledge. 1998. The DNA replication and damage checkpoint pathways induce transcription by inhibition of the Crt1 repressor. *Cell* 94:595–605.
19. James, P., J. Halladay, and E. A. Craig. 1996. Genomic libraries and a host strain designed for highly efficient two-hybrid selection in yeast. *Genetics* 144:1425–1436.
20. Jordan, A., and P. Reichard. 1998. Ribonucleotide reductases. *Annu. Rev. Biochem.* 67:71–98.
21. Koch, C., T. Moll, M. Neuberger, H. Ahorn, and K. Nasmyth. 1993. A role for the transcription factors Mbp1 and Swi4 in progression from G1 to S phase. *Science* 261:1551–1557.
22. Koshland, D., J. C. Kent, and L. H. Hartwell. 1985. Genetic analysis of the mitotic transmission of minichromosomes. *Cell* 40:393–403.
23. Kriwacki, R. W., L. Hengst, L. Tennant, S. I. Reed, and P. E. Wright. 1996. Structural studies of p21^{Waf1/Cip1/Sdi1} in the free and Cdk2-bound state: conformational disorder mediates binding diversity. *Proc. Natl. Acad. Sci. USA* 93:11504–11509.
24. Lozano, G., and S. J. Elledge. 2000. p53 sends nucleotides to repair DNA. *Nature* 404:24–25.
25. Ma, H., S. Kunes, P. J. Schatz, and D. Botstein. 1987. Plasmid construction by homologous recombination in yeast. *Gene* 58:201–216.
26. Matsuoka, S., M. Huang, and S. J. Elledge. 1998. Linkage of ATM to cell cycle regulation by the Chk2 protein kinase. *Science* 282:1893–1897.
27. Ouspenski, I. I., S. J. Elledge, and B. R. Brinkley. 1999. New yeast genes important for chromosome integrity and segregation identified by dosage effects on genome stability. *Nucleic Acids Res.* 27:3001–3008.
28. Parker, N. J., C. G. Begley, and R. M. Fox. 1991. Human M1 subunit of ribonucleotide reductase: cDNA sequence and expression in stimulated lymphocytes. *Nucleic Acids Res.* 19:3741.
29. Reichard, P. 1988. Interactions between deoxyribonucleotide and DNA synthesis. *Annu. Rev. Biochem.* 57:349–374.
30. Roman, H. 1956. Studies of gene mutation in *Saccharomyces*. *Gold Spring Harbor Symp. Quant. Biol.* 21:175–185.
31. Sattler, M., J. Schleucher, and C. Griesinger. 1999. Heteronuclear multidimensional NMR experiments for the structure determination of proteins in solution employing pulsed field gradients. *Prog. Nucl. Magn. Reson. Spectrosc.* 34:93–158.
32. Tanaka, H., H. Arakawa, T. Yamaguchi, K. Shiraishi, S. Fukuda, K. Matsui, Y. Takei, and Y. Nakamura. 2000. A ribonucleotide reductase gene involved in a p53-dependent cell-cycle checkpoint for DNA damage. *Nature* 404:42–49.
33. Wishart, D. S., C. G. Bigam, A. Holm, R. S. Hodges, and B. D. Sykes. 1995. ¹H, ¹³C and ¹⁵N random coil NMR chemical shifts of the common amino acids. I. Investigations of nearest-neighbor effects. *J. Biomol. NMR* 5:67–81.
34. Wright, P. E., and H. J. Dyson. 1999. Intrinsically unstructured proteins: re-assessing the protein structure-function paradigm. *J. Mol. Biol.* 293:321–331.
35. Zhao, X., E. G. Muller, and R. Rothstein. 1998. A suppressor of two essential checkpoint genes identifies a novel protein that negatively affects dNTP pools. *Mol. Cell* 2:329–340.
36. Zhou, Z., and S. J. Elledge. 1993. *DUN1* encodes a protein kinase that controls the DNA damage response in yeast. *Cell* 75:1119–1127.